

November 8, 2018

Observation of the h_b states and Beyond

A.E. BONDAR

*Budker Institute of Nuclear Physics, Novosibirsk, 630090, Russia
On behalf of Belle Collaboration*

Abstract

Originally designed for CP violation studies in the B meson system, the B-Factories recently showed an exciting capability for improving our experimental knowledge in the field of hadron spectroscopy. We review results on bottomonium spectroscopy from the Belle experiment at the KEK-B e^+e^- collider and present exciting new results from the unique large data set taken at the $\Upsilon(5S)$ resonance.

PRESENTED AT

The Ninth International Conference on
Flavor Physics and CP Violation
(FPCP 2011)
Maale Hachamisha, Israel, May 23–27, 2011

arXiv:1109.4476v1 [hep-ex] 21 Sep 2011

1 Introduction

The Belle Collaboration has collected a large sample of e^+e^- collisions at the energy of the $\Upsilon(5S)$ resonance, which lies above the threshold for production of B_s meson pairs, primarily with a purpose of studying decays of B_s . There have been a number of unexpected results on the non- $B_s\bar{B}_s$ decays of the $\Upsilon(5S)$. In particular, anomalously large rates for dipion transitions to lower bottomonium states $\Upsilon(5S) \rightarrow (\Upsilon(1S), \Upsilon(2S), \Upsilon(3S))\pi^+\pi^-$ have been observed [1]. If these signals are attributed entirely to the $\Upsilon(5S)$ decays, the measured partial decay widths $\Gamma[\Upsilon(5S) \rightarrow \Upsilon(nS)\pi^+\pi^-] \sim 0.5$ MeV are about two orders of magnitude larger than typical widths for dipion transitions among $\Upsilon(nS)$ states with $n \leq 4$.

Recently the CLEO-c Collaboration observed the process $e^+e^- \rightarrow h_c(1P)\pi^+\pi^-$ at a rate comparable to the process $e^+e^- \rightarrow J/\psi\pi^+\pi^-$ at $\sqrt{s} = 4170$ MeV and found an indication of an even higher transition rate at the $Y(4260)$ energy [2]. This implies that the $h_b(mP)$ production might be enhanced in the region of the Y_b and motivates a search for the $h_b(mP)$ in the $\Upsilon(5S)$ data.

We use the full $\Upsilon(5S)$ data sample with the integrated luminosity of 121.4 fb^{-1} collected near the peak of the $\Upsilon(5S)$ resonance with the Belle detector [3] at the KEKB asymmetric-energy e^+e^- collider [4].

2 Observation of the $h_b(1P)$ and $h_b(2P)$

We observe the $h_b(1P)$ and $h_b(2P)$ in the missing mass spectrum of $\pi^+\pi^-$ pairs. The $\pi^+\pi^-$ missing mass is defined as $MM(\pi^+\pi^-) \equiv \sqrt{(E_{c.m.} - E_{\pi^+\pi^-}^*)^2 - p_{\pi^+\pi^-}^{*2}}$, where $E_{c.m.}$ is the center-of-mass (c.m.) energy, $E_{\pi^+\pi^-}^*$ and $p_{\pi^+\pi^-}^*$ are the $\pi^+\pi^-$ energy and momentum measured in c.m. frame. The details of the analysis can be found in [5]. The $MM(\pi^+\pi^-)$ distribution for the selected $\pi^+\pi^-$ pairs is shown in Fig. 1(a). In this figure only the $\Upsilon(5S) \rightarrow \Upsilon(1S)\pi^+\pi^-$ and $\Upsilon(5S) \rightarrow \Upsilon(2S)\pi^+\pi^-$ transitions are discernible.

To fit the $MM(\pi^+\pi^-)$ spectrum, we separate it into three adjacent regions with boundaries at $MM(\pi^+\pi^-) = 9.3\text{ GeV}/c^2$, $9.8\text{ GeV}/c^2$, $10.1\text{ GeV}/c^2$ and $10.45\text{ GeV}/c^2$. We fit every region separately to better control the complicated shape of the combinatorial background, which is described by a Chebyshev polynomial of 6-7th order. In region 3 we subtract the K_S^0 contribution bin-by-bin, while in other regions its shape is smooth and is absorbed into combinatorial background. The signal peaks are described by Gaussians with parameters obtained from exclusive decays of the $\Upsilon(nS)$ to $\mu^+\mu^-$. The $MM(\pi^+\pi^-)$ spectrum with the combinatorial background and K_S^0 contributions subtracted, and the signal function resulting from the fit overlaid, are shown in Fig. 1(b). The significance of the $h_b(1P)$ and $h_b(2P)$ signals which includes the systematic uncertainty is 5.5σ and 11.2σ , respectively.

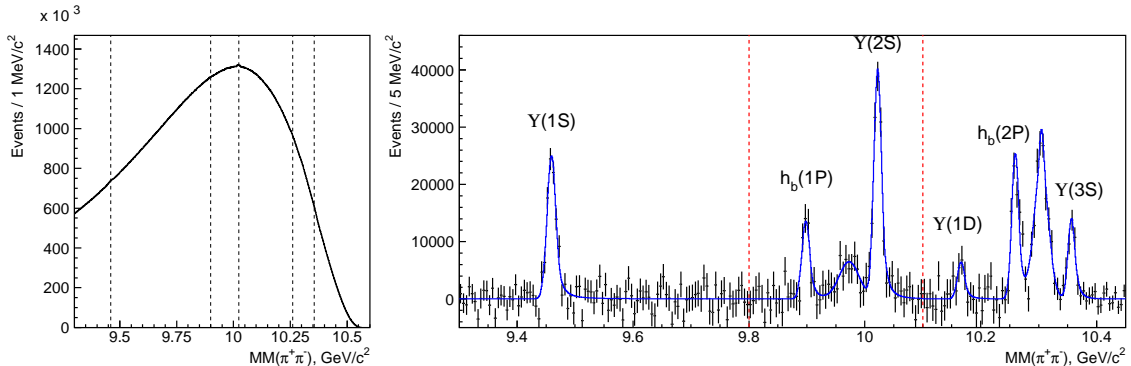


Figure 1: (a) The $MM(\pi^+\pi^-)$ distribution for the selected $\pi^+\pi^-$ pairs. Vertical lines indicate the locations of the $\Upsilon(1S)$, $h_b(1P)$, $\Upsilon(2S)$, $h_b(2P)$ and $\Upsilon(3S)$ signals. (b) The $MM(\pi^+\pi^-)$ spectrum with the combinatorial background and K_S^0 contributions subtracted (dots with error bars) and signal component of the fit function (solid histogram). The vertical dashed lines indicate the boundaries of the fit regions.

This is the first observation of the $h_b(1P)$ and $h_b(2P)$ spin-singlet bottomonium states in the reaction $e^+e^- \rightarrow h_b(mP)\pi^+\pi^-$ at the $\Upsilon(5S)$ energy. We measure the masses and the cross sections relative to the $e^+e^- \rightarrow \Upsilon(2S)\pi^+\pi^-$ cross-section: $M = 9898.25 \pm 1.06_{-1.07}^{+1.03}$ MeV/ c^2 , $R = 0.407 \pm 0.079_{-0.076}^{+0.043}$ for the $h_b(1P)$ and $M = 10259.76 \pm 0.64_{-1.03}^{+1.43}$ MeV/ c^2 , $R = 0.78 \pm 0.09_{-0.10}^{+0.22}$ for the $h_b(2P)$. The masses do not differ significantly from the center-of-gravity of the corresponding χ_{bJ} states. For the hyperfine splitting we find $\Delta M_{\text{HF}} = 1.62 \pm 1.52$ MeV/ c^2 for the $h_b(1P)$ and $0.48_{-1.22}^{+1.57}$ MeV/ c^2 for the $h_b(2P)$.

The values of R comparable with unity indicate that the $h_b(1P)$ and $h_b(2P)$ are produced via an exotic process that violates the suppression of heavy quark spin-flip. For further study we investigate resonant substructure of these decays [6]. Because of high background Dalitz plot analysis is impossible with current statistics, therefore we study the one-dimensional distributions in $M(h_b(mP)\pi)$. We define the $M(h_b(mP)\pi^+)$ as a missing mass of the opposite-sign pion, $MM(\pi^-)$. We measure the yield of signal decays as a function of the $MM(\pi^\pm)$ by fitting the $MM(\pi^+\pi^-)$ spectra in the bins of $MM(\pi^\pm)$. We combine the $MM(\pi^+\pi^-)$ spectra for the corresponding $MM(\pi^+)$ and $MM(\pi^-)$ bins and we use half of the phase space to avoid double counting.

Results of the fits for the $h_b(1P)$ yield as a function of $MM(\pi)$ are shown in Fig. 2. The $h_b(1P)$ yield exhibits a clear two-peak structure without any significant non-resonant contribution. In the following we refer to these structures as $Z_b(10610)$ and $Z_b(10650)$, respectively.

We perform a χ^2 fit to the $MM(\pi)$ distributions. We assume that spin-parity for both $Z_b(10610)$ and $Z_b(10650)$ is $J^P = 1^+$, therefore in the fit function we use a

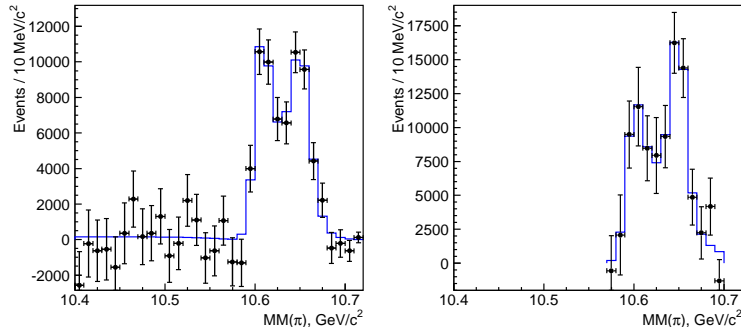


Figure 2: Left: the yield of the $h_b(1P)$ as a function of $MM(\pi)$ (points with error bars) and results of the fit (histogram). Right: the yield of the $h_b(2P)$ as a function of $MM(\pi)$ (points with error bars) and results of the fit (histogram).

coherent sum of two P -wave Breit-Wigner amplitudes; we add also a non-resonant contribution.

$$f = A |BW(s, M_1, \Gamma_1) + ae^{i\phi} BW(s, M_2, \Gamma_2) + be^{i\psi}|^2 \frac{qp}{\sqrt{s}}. \quad (1)$$

Here $\sqrt{s} \equiv MM(\pi)$; the variables A , M_k , Γ_k ($k = 1, 2$), a , ϕ , b and ψ are floating in the fit; $\frac{qp}{\sqrt{s}}$ is a phase-space factor, p (q) is the momentum of the pion originating from the $\Upsilon(5S)$ (Z_b) decay measured in the rest frame of the corresponding mother particle. The results of the fit are shown in Fig. 2 and are summarized in Table 1. The non-resonant amplitude is found to be consistent with zero. We find that the hypothesis of two resonances is favored over the hypothesis of a single resonance (no resonances) at the 7.4σ (17.9σ) level. The parameters of the $Z_b(10610)$ and $Z_b(10650)$ obtained in the fit of $h_b(1P)$ and $h_b(2P)$ are consistent with each other.

3 Analysis of $\Upsilon(5S) \rightarrow \Upsilon(1S, 2S, 3S)\pi^+\pi^-$

To select $\Upsilon(5S) \rightarrow \Upsilon(nS)\pi^+\pi^-$ candidate events we require the presence of a pair of muon candidates with an invariant mass in the range of $8.0 \text{ GeV}/c^2 < M(\mu^+\mu^-) < 11.0 \text{ GeV}/c^2$ and two pion candidates of opposite charge. These tracks are required to be consistent with coming from the interaction point. We also require that none of the four tracks be positively identified as an electron. No additional requirements are applied at this stage.

Candidate $\Upsilon(5S) \rightarrow \Upsilon(nS)\pi^+\pi^-$ events are identified by the invariant mass of the $\mu^+\mu^-$ combination and the missing mass $MM(\pi^+\pi^-)$ associated with the $\pi^+\pi^-$ system calculated as $MM(\pi^+\pi^-) = \sqrt{(E_{c.m.} - E_{\pi^+\pi^-}^*)^2 - p_{\pi^+\pi^-}^{*2}}$, where $E_{c.m.}$ is the

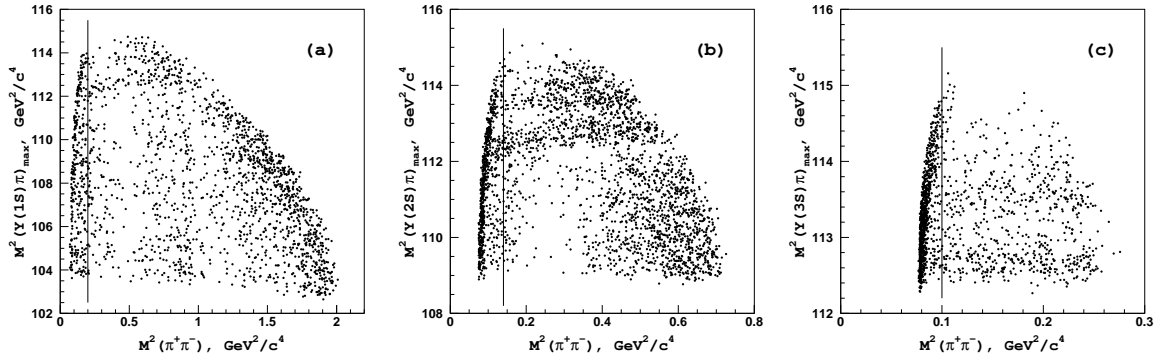


Figure 3: Dalitz plots for $\Upsilon(nS)\pi^+\pi^-$ events in the (a) $\Upsilon(1S)$; (b) $\Upsilon(2S)$; (c) $\Upsilon(3S)$ signal regions. Dalitz plot regions to the right of the vertical lines are included in the amplitude analysis.

center-of-mass (c.m.) energy and $E_{\pi^+\pi^-}^*$ and $p_{\pi^+\pi^-}^*$ are the energy and momentum of the $\pi^+\pi^-$ system measured in the c.m. frame.

The amplitude analyses of the three-body $\Upsilon(5S) \rightarrow \Upsilon(nS)\pi^+\pi^-$ decays that are reported here are performed by means of unbinned maximum likelihood fits to two-dimensional Dalitz distributions.

Before fitting the Dalitz plot for events in the signal region, we determine the distribution of background events over the Dalitz plot using events in the $\Upsilon(nS)$ mass sidebands that are refitted to the nominal mass of the corresponding $\Upsilon(nS)$ state to match the phase space boundaries.

In the sideband Dalitz distributions one can see a strong concentration of background events in the very low $\pi^+\pi^-$ invariant mass region; these are due to photon conversion on the innermost parts of the Belle detector. Because of their low energy, these conversion electrons are poorly identified and pass the electron veto requirement. We exclude this high background region by applying the requirements on the $\pi^+\pi^-$ invariant mass. For the remainder of the Dalitz plot the distribution of background events is assumed to be uniform. The variation of reconstruction efficiency across the Dalitz plot is determined from MC simulation. The fraction of signal events in the signal region for each of the three $\Upsilon(nS)\pi^+\pi^-$ final states is determined from a fit to the corresponding $MM(\pi^+\pi^-)$ spectrum using a Crystal Ball function [7] for the Υ signal and a linear function for the combinatorial background component.

Figure 3 shows Dalitz plots of the events in the signal regions for the three decay channels under study. In all cases, two horizontal bands are evident in the $\Upsilon(nS)\pi$ system near $10.61 \text{ GeV}/c^2$ ($\sim 112.6 \text{ GeV}^2/c^4$) and $10.65 \text{ GeV}/c^2$ ($\sim 113.3 \text{ GeV}^2/c^4$).

We use the following parameterization for the $\Upsilon(5S) \rightarrow \Upsilon(nS)\pi^+\pi^-$ three-body decay amplitude:

$$M(s_1, s_2) = A_1(s_1, s_2) + A_2(s_1, s_2) + A_{f_0} + A_{f_2} + A_{NR}, \quad (2)$$

where $s_1 = M^2(\Upsilon(nS)\pi^+)$, $s_2 = M^2(\Upsilon(nS)\pi^-)$. Here we assume that the dominant contributions come from the amplitudes that conserve the orientation of the spin of the heavy quarkonium state and, thus, both pions in the cascade decay $\Upsilon(5S) \rightarrow Z_b\pi \rightarrow \Upsilon(nS)\pi^+\pi^-$ are emitted in an S -wave with respect to the heavy quarkonium system. As will be shown later, angular analyses support this assumption. Consequently, we parameterize the observed $Z_b(10610)$ and $Z_b(10650)$ peaks with an S -wave Breit-Wigner function without s dependence of the resonance width Γ . To account for the possibility of $\Upsilon(5S)$ decay to both $Z^+\pi^-$ and $Z^-\pi^+$, the amplitudes A_1 and A_2 are symmetrized with respect to π^+ and π^- transposition. Taking into account isospin symmetry, the resulting amplitude is written as

$$A_k(s_1, s_2) = a_k e^{i\delta_k} (BW(s_1, M_k, \Gamma_k) + BW(s_2, M_k, \Gamma_k)), \quad (3)$$

where the masses M_k and the widths Γ_k ($k = 1, 2$) are free parameters of the fit. Due to the very limited phase space available in the $\Upsilon(5S) \rightarrow \Upsilon(3S)\pi^+\pi^-$ decay, there is a significant overlap between the two processes $\Upsilon(5S) \rightarrow Z_b^+\pi^-$ and $\Upsilon(5S) \rightarrow Z_b^-\pi^+$. We also include amplitudes A_{f_0} and A_{f_2} to account for possible contributions in the $\pi^+\pi^-$ channel from $f_0(980)$ scalar and $f_2(1270)$ tensor states, respectively. Inclusion of the $f_0(980)$ state is necessary in order to describe the prominent structure in the $M(\pi^+\pi^-)$ spectrum for the $\Upsilon(1S)\pi^+\pi^-$ final state around $M(\pi^+\pi^-) = 1.0 \text{ GeV}/c^2$ (see Fig. 4). We also find that the addition of the $f_2(1270)$ gives a better description of the data at $M(\pi^+\pi^-) > 1.0 \text{ GeV}/c^2$ and drastically improves the fit likelihood values. We use a Breit-Wigner function to parameterize the $f_2(1270)$ and a coupled-channel Breit-Wigner (Flatte) function [8] for the $f_0(980)$. The mass and the width of the $f_2(1270)$ state are fixed at their world average values [9]; the mass and the coupling constants of the $f_0(980)$ state are fixed at values defined from the analysis of $B^+ \rightarrow K^+\pi^+\pi^-$: $M(f_0(980)) = 950 \text{ MeV}/c^2$, $g_{\pi\pi} = 0.23$, $g_{KK} = 0.73$ [10].

Following suggestions given in Refs.[11] and references therein, the non-resonant amplitude A_{NR} has been parameterized as

$$A_{NR} = a_1^{\text{nr}} \cdot e^{i\delta_1^{\text{nr}}} + a_2^{\text{nr}} \cdot e^{i\delta_2^{\text{nr}}} \cdot s_3, \quad (4)$$

where $s_3 = M^2(\pi^+\pi^-)$ (s_3 is not an independent variable and can be expressed via s_1 and s_2 but we use it here for clarity), a_1^{nr} , a_2^{nr} , δ_1^{nr} and δ_2^{nr} are free parameters of the fit (with an exception of the $\Upsilon(3S)\pi^+\pi^-$ channel as described below).

The logarithmic likelihood function \mathcal{L} is then constructed as

$$\mathcal{L} = -2 \sum \log(f_{\text{sig}}S(s_1, s_2) + (1 - f_{\text{sig}})B(s_1, s_2)), \quad (5)$$

where $S(s_1, s_2) = |M(s_1, s_2)|^2$ folded with the detector resolution function ($5.6 \text{ MeV}/c^2$ for $M(\Upsilon(nS)\pi^\pm)$; the $M(\pi^+\pi^-)$ resolution is better and is not taken into account since no narrow resonances are observed in the $\pi^+\pi^-$ system), $B(s_1, s_2) = 1$ and f_{sig} is a

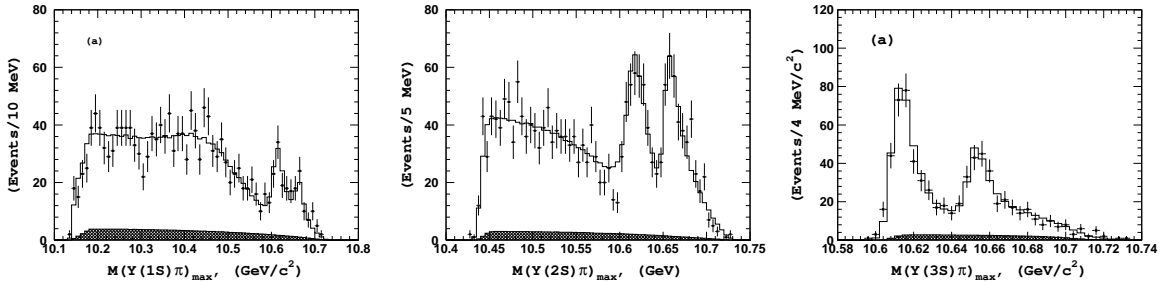


Figure 4: Comparison of fit results (open histogram) with experimental data (points with error bars) for events in the $\Upsilon(1S)$, $\Upsilon(2S)$ and $\Upsilon(3S)$ signal regions. The hatched histogram shows the background component.

fraction of signal events in the data sample. Both $S(s_1, s_2)$ and $B(s_1, s_2)$ are corrected for reconstruction efficiency.

In the fit to the $\Upsilon(1S)\pi^+\pi^-$ sample, the amplitudes and phases of all of the components are allowed to float. However, in the cases of $\Upsilon(2S)\pi^+\pi^-$ and $\Upsilon(3S)\pi^+\pi^-$ the available phase space is significantly smaller and contributions from the $f_0(980)$ and $f_2(1270)$ are not well defined. Thus, in the fit to the $\Upsilon(2S)\pi^+\pi^-$ and $\Upsilon(3S)\pi^+\pi^-$ signal samples, we fix the amplitudes and relative phases of these components to the values measured in the fit to the $\Upsilon(1S)\pi^+\pi^-$ sample. Moreover, in the fit to the $\Upsilon(3S)\pi^+\pi^-$ sample, we also fix the a_2^{nr} and δ_2^{nr} parameters of the A_{nr} amplitude. Possible effects of these assumptions are considered while determining the model-dependent uncertainty. Results of the fits to $\Upsilon(5S) \rightarrow \Upsilon(nS)\pi^+\pi^-$ signal events are shown in Fig. 4, where one-dimensional projections of the data and fits are compared. To combine Z_b^+ and Z_b^- events we plot $\Upsilon(nS)\pi$ mass distributions in terms of $M(\Upsilon(nS)\pi)_{\text{min}}$ and $M(\Upsilon(nS)\pi)_{\text{max}}$; fits are performed in terms of $M(\Upsilon(nS)\pi^+)$ and $M(\Upsilon(nS)\pi^-)$. Results of the fits are summarized in Table 1. We try various alternative models to parameterize the decay amplitude as described in the systematic uncertainty section. The combined statistical significance of the two peaks exceeds 10 sigma for all tested models and for all $\Upsilon(nS)\pi^+\pi^-$ channels.

4 Discussion and Conclusions

In conclusion, we have observed two charged bottomonium-like resonances, the $Z_b(10610)$ and $Z_b(10650)$, with signals in five different decay channels, $\Upsilon(nS)\pi^\pm$ ($n = 1, 2, 3$) and $h_b(mP)\pi^\pm$ ($m = 1, 2$). Parameters of the resonances as measured in different channels are summarized in Table 1. All channels yield consistent results as can be seen in Fig. 5. A simple weighted averages over all five channels give $M[Z_b(10610)] = 10608.4 \pm 2.0 \text{ MeV}/c^2$, $\Gamma[Z_b(10610)] = 15.6 \pm 2.5 \text{ MeV}$ and $M[Z_b(10650)] = 10653.2 \pm$

Table 1: Comparison of results on $Z_b(10610)$ and $Z_b(10650)$ parameters obtained from $\Upsilon(5S) \rightarrow \Upsilon(nS)\pi^+\pi^-$ ($n = 1, 2, 3$) and $\Upsilon(5S) \rightarrow h_b(mP)\pi^+\pi^-$ ($m = 1, 2$) analyses. Quoted values are in MeV/c^2 for masses, in MeV for widths and in degrees for the relative phase. Relative amplitude is defined as $a_{Z_b(10650)}/a_{Z_b(10610)}$.

Final state	$\Upsilon(1S)\pi^+\pi^-$	$\Upsilon(2S)\pi^+\pi^-$	$\Upsilon(3S)\pi^+\pi^-$	$h_b(1P)\pi^+\pi^-$	$h_b(2P)\pi^+\pi^-$
$M(Z_b(10610))$	$10609 \pm 3 \pm 2$	$10616 \pm 2^{+3}_{-4}$	$10608 \pm 2^{+5}_{-2}$	$10605.1 \pm 2.2^{+3.0}_{-1.0}$	$10596 \pm 7^{+5}_{-2}$
$\Gamma(Z_b(10610))$	$22.9 \pm 7.3 \pm 2$	$21.1 \pm 4^{+2}_{-3}$	$12.2 \pm 1.7 \pm 4$	$11.4^{+4.5+2.1}_{-3.9-1.2}$	16^{+16+13}_{-10-4}
$M(Z_b(10650))$	$10660 \pm 6 \pm 2$	$10653 \pm 2 \pm 2$	$10652 \pm 2 \pm 2$	$10654.5 \pm 2.5^{+1.0}_{-1.9}$	$10651 \pm 4 \pm 2$
$\Gamma(Z_b(10650))$	$12 \pm 10 \pm 3$	$16.4 \pm 3.6^{+4}_{-6}$	$10.9 \pm 2.6^{+4}_{-2}$	$20.9^{+5.4+2.1}_{-4.7-5.7}$	12^{+11+8}_{-9-2}
Rel. amplitude	$0.59 \pm 0.19^{+0.09}_{-0.03}$	$0.91 \pm 0.11^{+0.04}_{-0.03}$	$0.73 \pm 0.10^{+0.15}_{-0.05}$	$1.8^{+1.0+0.1}_{-0.7-0.5}$	$1.3^{+3.1+0.4}_{-1.1-0.7}$
Rel. phase,	$53 \pm 61^{+5}_{-50}$	$-20 \pm 18^{+14}_{-9}$	$6 \pm 24^{+23}_{-59}$	188^{+44+4}_{-58-9}	$255^{+56+12}_{-72-183}$

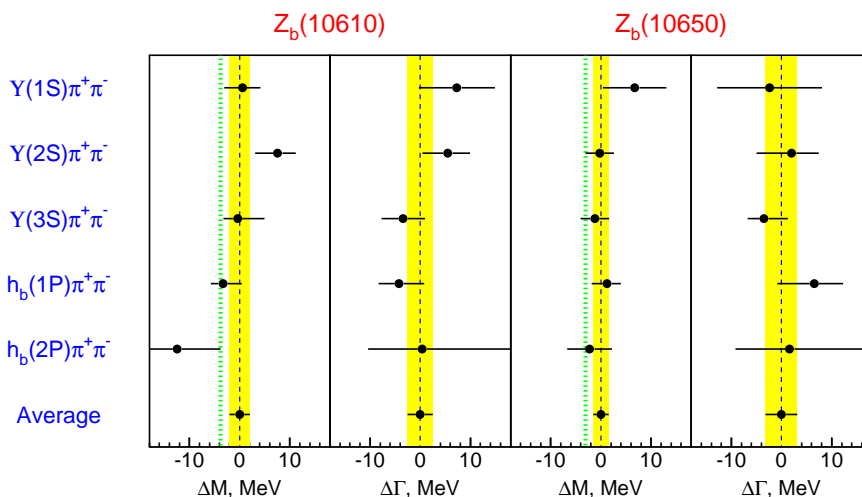


Figure 5: Comparison of $Z_b(10610)$ and $Z_b(10650)$ parameters obtained from different decay channels. The vertical dotted lines indicate $B^*\bar{B}$ and $B^*\bar{B}^*$ thresholds.

$1.5 \text{ MeV}/c^2$, $\Gamma[Z_b(10650)] = 14.4 \pm 3.2 \text{ MeV}$, where statistical and systematic errors are added in quadrature.

The measured masses of these states exceed by only a few MeV/c^2 the thresholds for the open beauty channels $B^*\bar{B}$ (10604.6 MeV) and $B^*\bar{B}^*$ (10650.2 MeV). This “coincidence” can be explained by a molecular-like type of new states, *i.e.*, their structure is determined by the strong interaction dynamics of the $B^*\bar{B}$ and $B^*\bar{B}^*$ meson pairs [12].

The widths of both states are similar and are of the order of $15 \text{ MeV}/c^2$. The $Z_b(10610)$ production rate is similar to the $Z_b(10650)$ production rate for every decay channel. Their relative phase is consistent with zero for the final states with the $\Upsilon(nS)$ and consistent with 180 degree for the final states with the $h_b(mP)$.

The $\Upsilon(5S) \rightarrow h_b(mP)\pi^+\pi^-$ decays seem to be saturated by the $Z_b(10610)$ and

$Z_b(10650)$ intermediate states; this decay mechanism is responsible for the high rate of the $\Upsilon(5S) \rightarrow h_b(mP)\pi^+\pi^-$ process measured recently by the Belle Collaboration.

Analysis of angular distributions for charged pions [6] favors the $J^P = 1^+$ spin-parity assignment for both $Z_b(10610)$ and $Z_b(10650)$. Since the $\Upsilon(5S)$ has negative G-parity, Z_b states will have opposite G-parity due to emission of the pion.

References

- [1] K.-F. Chen *et al.* (Belle Collaboration), Phys. Rev. Lett. **100**, 112001 (2008).
- [2] R.E. Mitchell, arXiv:1102.3424v1.
- [3] A. Abashian *et al.* (Belle Collaboration), Nucl. Instrum. Methods Phys. Res., Sect. A **479**, 117 (2002).
- [4] S. Kurokawa and E. Kikutani, Nucl. Instrum. Methods Phys. Res. Sect., **A499**, 1 (2003), and other papers included in this Volume.
- [5] I. Adachi *et al.* (Belle Collaboration) arXiv:1103.3419.
- [6] I. Adachi *et al.* (Belle Collaboration) arXiv:1105.4583.
- [7] T. Skwarnicki, Ph.D. Thesis, Institute for Nuclear Physics, Krakow 1986; DESY Internal Report, DESY F31-86-02 (1986).
- [8] S.M. Flatté, Phys. Lett. B **63**, 224, (1976).
- [9] K. Nakamura *et al.* (Particle Data Group), J. Phys. **G 37**, 075021 (2010).
- [10] A. Garmash *et al.* (Belle Collaboration), Phys. Rev. Lett. **96**, 251803 (2006).
- [11] M.B. Voloshin, Prog. Part. Nucl. Phys. **61**, 455 (2008).
M.B. Voloshin, Phys. Rev. D **74**, 054022 (2006).
- [12] A.E. Bondar *et al.* arXiv:1105.4473,
M.B. Voloshin arXiv:1105.5829.